Critical behavior of weak itinerant ferromagnet $Fe_{90-x}Mn_xZr_{10}$ $(0 \leqslant x \leqslant 16)$ alloys

A. Perumal* and V. Srinivas†
Department of Physics and Meteorology, Indian Institute of Technology, Kharagpur, 721 302, India
(Received 8 August 2002; published 24 March 2003)

The magnetic behavior of amorphous $Fe_{90-x}Mn_xZr_{10}$ $(0 \leqslant x \leqslant 16)$ alloys has been investigated in the critical region from which we determined the Curie temperature (T_c) and critical exponents (γ, β, and δ). Detailed analysis suggests that the exponents are asymptotic and independent of the method of analysis in the actual critical region (ACR), while it strongly depends on the method of analysis outside the ACR. Asymptotic critical exponent values are very close to those predicted by a three-dimensional nearest-neighbor Heisenberg model. The obtained results provide strong experimental evidence of *weak itinerant* ferromagnetism.

DOI: 10.1103/PhysRevB.67.094418 PACS number(s): 75.40.Cx, 07.55.Jg, 51.60.+a, 75.50.Lk

Randomly diluted magnetic systems with short-range interactions have captured the attention of scientists in recent years.[1] Heuristic arguments and renormalization group (RG) calculations[2] assert that the critical behavior near the ferromagnetic (FM) to paramagnetic (PM) phase transition of a pure spin system with negative specific heat critical exponent (α) does not get altered by the presence of short-range quenched disorder.[3] For example, in the case of magnetic materials a careful analysis based on the simple power law (SPL) indicates that the critical regime spans a wide reduced temperature range $\eta[=(T-T_c)/T_c] \leqslant 0.04 \pm 0.02$ below which the critical exponents do not seem to vary with temperature. Moreover, critical phenomenon studies of a large number of systems[4] have testified to this in the past. However, it is surprising that the FM-PM phase transition at the Curie temperature (T_c) in many systems is characterized by the values of the critical exponents [β for spontaneous magnetization $\sigma_s(T)$, γ for initial susceptibility $\chi(T)$, and δ for critical isotherm $\sigma(H_{ex},T_c)$] that are considerably larger than[5] those theoretically predicted for an ordered three-dimensional (3D) nearest-neighbor (NN) isotropic Heisenberg ferromagnet.

Most of the theories of critical phenomena in magnets consider that these systems consist of magnetic moments (spins) localized at lattice sites and interacting with one another through exchange interactions. On the other hand, the theoretical models applicable to *itinerant* ferromagnets are restricted to only three models: (i) the Heisenberg spin system with long-range dipolar[6] interactions, (ii) the *d-dimensional* spin system with an isotropic *n-component* order parameter,[7] (iii) the spherical model[8] version (i.e., $n \rightarrow \infty$) of (ii). Experimental studies of the critical behavior of *weak itinerant* ferromagnets have been confined to only a few systems[9] and rarely more than two critical exponents have been determined. Moreover, a close scrutiny of the results published in the literature reveals that the obtained exponents may suffer from one of the following problems: (a) the values of the critical exponents are found to vary with the scaling equation of state, and (b) due to the nonlinearity in the magnetization curve at higher fields, the extrapolation method obviously leads to large uncertainties in the zero-field quantities and hence the critical exponents.

Here, we report a detailed analysis of the critical behavior of a series of amorphous (a-)$Fe_{90-x}Mn_xZr_{10}$ $(0 \leqslant x \leqslant 16)$ alloys based on various methods to resolve the issues that are highlighted above and to answer some basic questions that have been unanswered until now: (a) Which model forms the most appropriate theoretical description of the critical-point behavior of *weak itinerant* ferromagnets? (b) Do *weak itinerant* electron ferromagnets fall naturally into one of the known universality classes of critical phenomena or do they form a class of their own? The choice of the present series has been dictated by the fact that this series exhibits reentrant behavior over a wide composition range[10] and also to verify a recent analysis of magnetization data on FeMnZr alloys that gave extremely large values of the critical exponents compared to the 3D NN Heisenberg model.

Amorphous $Fe_{90-x}Mn_xZr_{10}$ alloys ($x=0$, 4, 6, 8, 10, 12, and 16) were prepared by the conventional melt-spinning

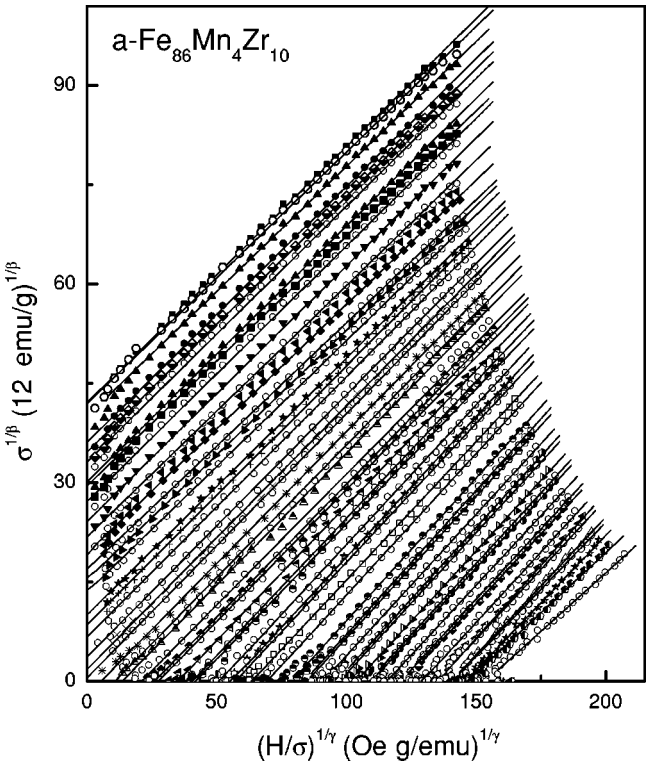

FIG. 1. Modified Arrott plot [$\sigma^{1/\beta}$ vs $(H/\sigma)^{1/\gamma}$] for amorphous $Fe_{86}Mn_4Zr_{10}$ alloy. Note that only three-fourths of the actual data are shown for the sake of clarity.

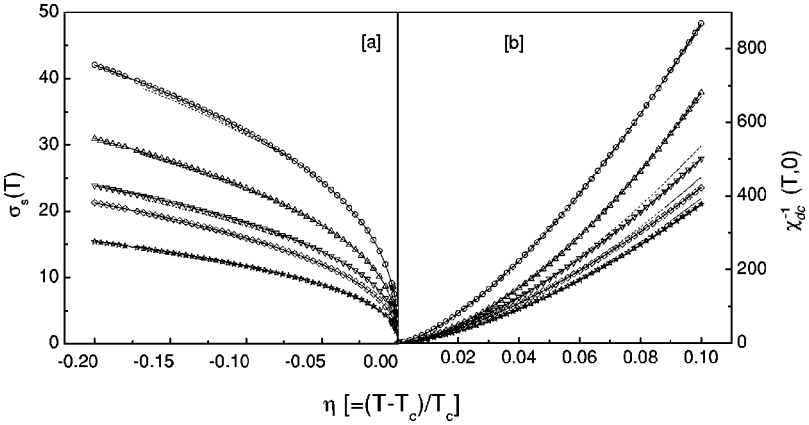

FIG. 2. (a) Spontaneous magnetization (σ_s) and (b) inverse susceptibility (χ_{dc}^{-1}) plotted against reduced temperature (η) for amorphous $Fe_{90-x}Mn_xZr_{10}$ ($x=0$, 4, 8, 10, and 12) alloys. The dashed and solid curves passing through the data points represent the best least-squares fit based on Eqs. (1c), (1d) and (2c), (2d), respectively.

technique in an argon atmosphere. Magnetization measurements were performed in external fields up to 50 kOe over a wide temperature range $0.6T_c \leqslant T \leqslant 1.4T_c$. In order to deduce T_c and the zero-field quantities $\sigma_s(T)$ and $\chi_{dc}^{-1}(T)$, the raw magnetization data are converted into $\sigma^{1/\beta}$ vs $(H/\sigma)^{1/\gamma}$ such that the data taken in the critical region fall on a set of straight lines through a choice of critical exponents β and γ.[11] The low-field ac susceptibility (ACS) measurement was carried out by the mutual inductance method at a frequency of 80 Hz in a rms field of 26 mOe. More details about the sample characterizations are given elsewhere.[11]

The typical modified Arrott plot (MAP), constructed out of raw σ-H isotherms, is shown in Fig. 1 for a-$Fe_{86}Mn_4Zr_{10}$ alloy. Note that only three-fourths of the actual data set is shown in figure for the clarity. This figure captures all the essential features for the remaining compositions. The $\sigma_s(T)$ and $\chi_{dc}^{-1}(T)$ were computed from the intercept values at different temperatures on the ordinate ($T \leqslant T_c$) and abscissa ($T \geqslant T_c$), when the linear high-field portion of the MAP plot is extrapolated to $\sigma^{1/\beta}=0$ and $(H/\sigma)^{1/\gamma}=0$, respectively, as shown in Fig. 1. At $T=T_c$, the MAP isotherm is linear over the entire σ/H range and upon extrapolation passes through the origin. The determined values of $\sigma_s(T)$ and $\chi_{dc}^{-1}(T)$ are plotted against η in Fig. 2. By contrast, low-field ACS is a direct measure of the intrinsic susceptibility and referred to as $\chi_{ac}(T)$. With a view to ascertain which theories of critical phenomena correctly describes the present system, $\sigma_s(T)$, $\chi_{dc}^{-1}(T)$, and $\chi_{ac}^{-1}(T)$ data were analyzed in terms of the following equations:

$$\sigma_s(T) = \sigma_0^{eff}(-\eta)^{\beta_{eff}}, \quad \eta < 0, \tag{1a}$$

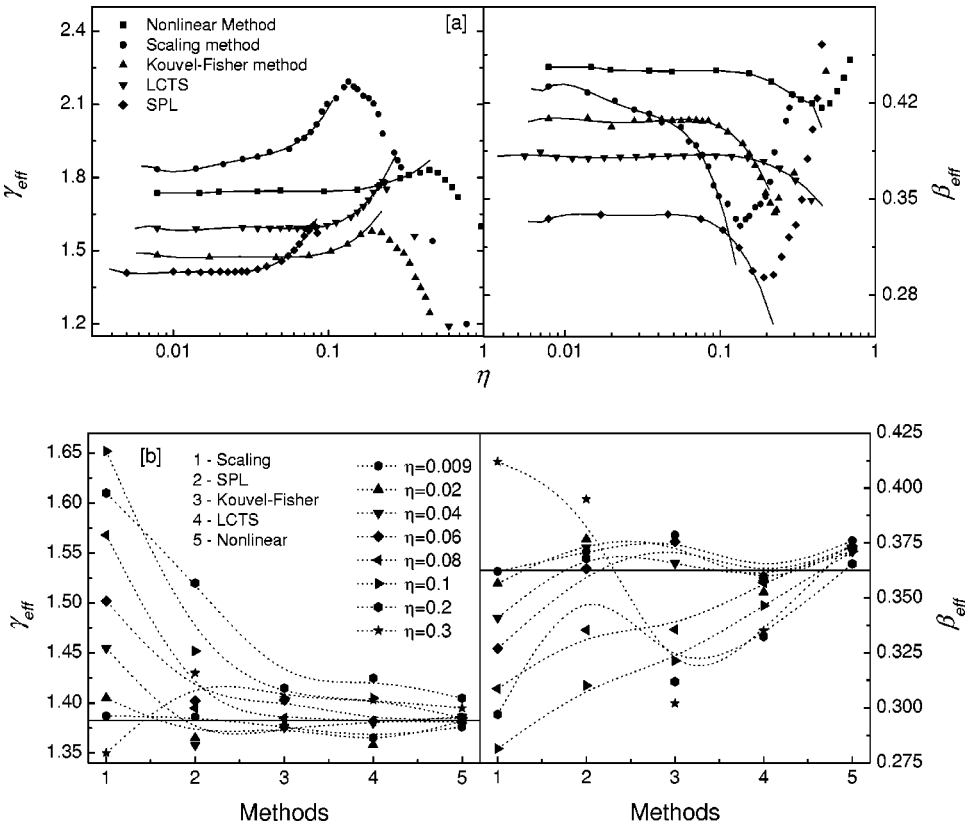

FIG. 3. (a) The effective exponent values of γ and β, obtained from various methods, plotted against the reduced temperature range. In order to show the variation clearly, the exponent value γ [β] is shifted vertically 0.09 [0.02] (Kouvel-Fisher method), 0.20 [0.03] (leading correction to scaling analysis), 0.36 [0.08] (Nonlinear method), and 0.5 [0.095] (scaling method) with respect to their actual variations. (b) The effective critical exponents obtained from various methods over different temperature ranges. The horizontal line in the figure indicates the theoretical values for 3D NN Heisenberg ferromagnets.

TABLE I. The determined values of the Curie temperature (T_c^-, T_c^0, T_c^+), critical exponents (γ, β), Curie-Weiss-like constant (C_χ), effective magnetic moment in the paramagnetic state (q_p), saturation magnetic moment (q_s), and the ratio of magnetic moments for amorphous $Fe_{90-x}Mn_xZr_{10}$ alloys. The parameters within the parentheses indicate the error in the parameter.

x	T_c^-	T_c^0	T_c^+	γ	β	C_χ (10^{-3})	q_p	q_s	q_p/q_s
0	226.5(4)	226.6(5)	226.4(3)	1.376(6)	0.369(4)	3.81(2)	6.341(7)	1.532(5)	4.139
4	214.2(7)	214.3(3)	214.2(4)	1.383(7)	0.373(8)	4.89(3)	7.099(6)	1.432(8)	4.957
6	197.1(6)	197.2(4)	197.1(7)	1.359(4)	0.358(6)	5.64(2)	7.280(8)	1.261(7)	5.773
8	184.8(7)	184.7(8)	185.6(6)	1.364(8)	0.355(5)	6.12(4)	7.404(8)	1.131(9)	6.546
10	169.3(6)	169.3(6)	169.1(8)	1.406(5)	0.356(3)	6.83(3)	7.862(5)	1.021(9)	7.700
12	154.1(8)	154.2(3)	154.1(9)	1.395(4)	0.376(4)	7.79(2)	8.887(4)	0.981(4)	9.062
16	131.2(6)	131.3(7)	131.2(3)	1.412(4)	0.362(2)	8.80(2)	10.231(4)	0.913(8)	11.206

$$\sigma_s(T)=\sigma_0(-\eta)^{\beta}[1+u_{\sigma_1}^{-}(-\eta)^{\Delta_1}+u_{\sigma_2}^{-}(-\eta)^{\Delta_2}],\quad \eta<0, \tag{1b}$$

$$\sigma_s(T)=\sigma_0'|\tilde{\eta}|^{\beta}[1+\tilde{u}_{\sigma_1}^{-}|\tilde{\eta}|^{\Delta_1}+\tilde{u}_{\sigma_2}^{-}|\tilde{\eta}|^{\Delta_2}],\quad \tilde{\eta}<0, \tag{1c}$$

$$\sigma_s(T)=\sigma_0''|\tilde{\eta}|^{\beta}[1+\tilde{u}_{\sigma}^{-}(|\tilde{\eta}|)],\quad \tilde{\eta}<0, \tag{1d}$$

$$\chi^{-1}(T)=z^{eff}\eta^{\gamma_{eff}},\quad \eta>0, \tag{2a}$$

$$\chi^{-1}(T)=z\eta^{\gamma}[1+u_{\chi_1}^{+}(\eta)^{\Delta_1}+u_{\chi_2}^{+}(\eta)^{\Delta_2}]^{-1},\quad \eta<0, \tag{2b}$$

$$\chi^{-1}(T)=z't\tilde{\eta}^{\gamma}[1+\tilde{u}_{\chi_1}^{+}(\tilde{\eta})^{\Delta_1}+\tilde{u}_{\chi_2}^{+}(\tilde{\eta})^{\Delta_2}]^{-1},\quad \tilde{\eta}<0, \tag{2c}$$

$$\chi^{-1}(T)=z''t\tilde{\eta}^{\gamma}[1+\tilde{u}_{\chi}^{+}(\tilde{\eta})]^{-1},\quad \tilde{\eta}<0, \tag{2d}$$

where, γ, β [Δ_1, Δ_2] are the critical exponents [leading correction to scaling (LCTS) exponents], $u_{\sigma_1}^{-}$, $u_{\sigma_2}^{-}$, $\tilde{u}_{\sigma_1}^{-}$, $\tilde{u}_{\sigma_2}^{-}$, $\tilde{u}_{\sigma}^{-}$, $u_{\chi_1}^{+}$, $u_{\chi_2}^{+}$, $\tilde{u}_{\chi_1}^{+}$, $\tilde{u}_{\chi_2}^{+}$, $\tilde{u}_{\chi}^{+}$, $z=(h_0/m_0)$ are the critical amplitudes, and $\tilde{\eta}=(t-1)/t$, $t=T/T_c$ are the nonlinear scaling variables. A detailed analysis of the $\sigma_s(T)$, $\chi_{dc}^{-1}(T)$, and $\chi_{ac}^{-1}(T)$ data based on Eqs. (1) and (2) reveals that in the asymptotic critical region (ACR), Eq. (1c) [(2c)] reproduces $\sigma_s(T)$ [$\chi^{-1}(T)$] data to a far greater accuracy than Eq. (1d) [(2d)]. In the ACR, the LCTS analysis based on the expressions that include the nonanalytic correction terms alone yields the same result regardless of whether these correction terms are expressed in linear scaling variables [Eqs. (1b) and (2b)] or in nonlinear scaling variables [Eqs. (1c) and (2c)]. On the other hand, Eqs. (1d) and (2d) provide very good overall fits in a temperature ranges as wide as $0.6T_c \leqslant T \leqslant T_c$ for $\sigma_s(T)$ and $T_c \leqslant T \leqslant 1.4T_c$ for $\chi^{-1}(T)$. Note that all independent determinations of the T_c's (T_c^-, T_c^+, and T_c^0) show more or less same value ($T_c^- \approx T_c^+ \approx T_c^0$) within the error limits.

The effective critical exponents β_{eff} and γ_{eff} were calculated[12] at different temperature ranges and are depicted in Fig. 3(a). A comparison between effective exponents and Eqs. (1b) and (2b) reveals that in the ACR ($|\eta|<|\eta_{cross}|$)[13], β_{eff} [γ_{eff}] and β [γ] are related as

$$\beta_{eff}(\eta)=\beta+u_{\sigma_1}^{-}\Delta_1(-\eta)^{\Delta_1}+u_{\sigma_2}^{-}\Delta_2(-\eta)^{\Delta_2}, \tag{3a}$$

$$\gamma_{eff}(\eta)=\gamma-u_{\chi_1}^{+}\Delta_1(\eta)^{\Delta_1}-u_{\chi_2}^{+}\Delta_2(\eta)^{\Delta_2}, \tag{3b}$$

and in the limit $(-\eta)\to 0^-$ [$\eta\to 0^+$], $\beta_{eff}(\eta)$ [$\gamma_{eff}(\eta)$] coincides with β [γ]. The obtained critical exponents β and γ by various methods in the different reduced temperature ranges are shown in Fig. 3(b). The determined critical exponents are independent of the method of analysis in the ACR, while it strongly depends on the method of analysis outside the ACR.

It is well known that in the present series of amorphous alloys, the spin-wave stiffness constant (D) renormalizes with temperature in accordance with the comparison predicted by both localized (Heisenberg) and itinerant models. The calculated value of the NN distance[14] is close to the values predicted for typical mean NN transition-metal–transition-metal distances in amorphous ferromagnets.[15] The local magnetic anisotropy and high-field susceptibility (χ_{hf}) are observed to increase with increasing Mn concentration.[16] The calculated value of χ_{hf} decreases rapidly as the temperature is lowered below T_c and goes through a broad minimum before attaining a constant value at low temperature, indicating the typical character of *weak itinerant* ferromagnets.[14,17] An elaborate analysis of the data reveals that (i) nonanalytic LCTS terms essentially control the temperature dependence of $\sigma_s(T)$ and $\chi^{-1}(T)$ data for temperatures close to T_c, and (ii) in the ACR, nonlinear scaling yields the same result as its linear counterpart does. Moreover, the single leading analytic correction term in nonlinear variables [Eq. (2d)] permit an unambiguous determination of the magnetic moment per alloy atom in the paramagnetic state, q_p, through the relation $q_p(q_p+2)=(2.828)^2(C_\chi A/\rho)$, where $C_\chi=(T_c/z'')$, and A and ρ are the atomic weight and density, respectively. The computed values of q_p and those of the ratio q_p/q_s (where q_s is the saturation magnetic moment per alloy atom at 0 K) are listed in Table I along with the values of the critical exponents. For all the amorphous alloys, the ratio $q_p/q_s \gg 1$ and it falls on a straight line when plotted against T_c^{-1} or

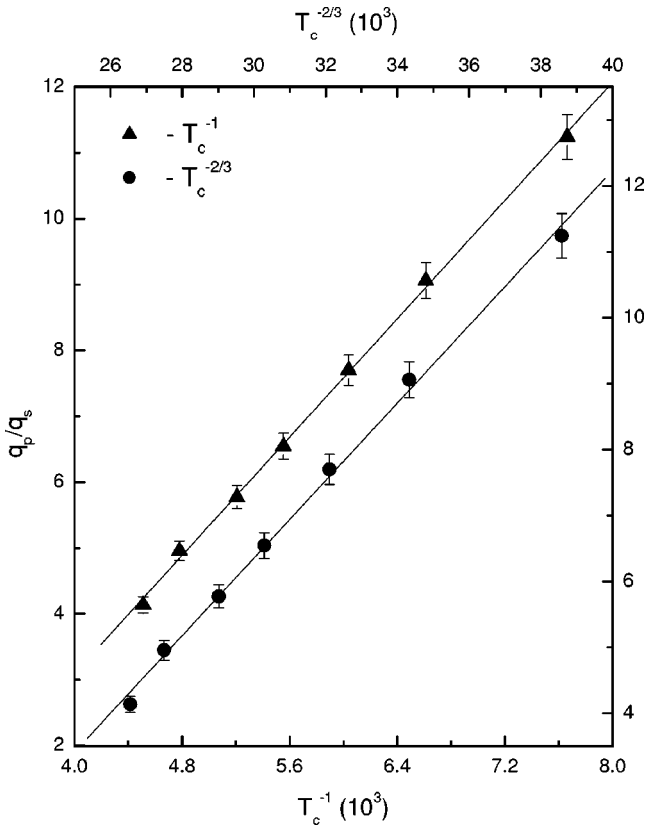

FIG. 4. The ratio of the magnetic moments, q_p/q_s, plotted against various temperature scales T_c^{-1} and $T_c^{-2/3}$. The solid lines passing through data points denote the best fit to the data.

$T_c^{-2/3}$, as shown in Fig. 4. According to the Rhodes-Wohlfarth criterion,[18] the greater the amount by which the q_p/q_s ratio exceeds unity, the more *itinerant* is the magnetic moment. These results are inadequate to make a clear-cut distinction between the two criteria because the range of T_c values that are covered in the present experiments is not wide enough. However, the present observation suggests that these *weak itinerant* ferromagnets behave like 3D NN Heisenberg ferromagnets in the critical region, when one considers in conjunction with the result of RG calculations[2] that for a d-dimensional spin system with an isotropic n-component order parameter and interactions $J(r)$ decaying as $J(r) = 1/a^{d+\sigma_{int}}(\sigma_{int}>0)$, the critical exponents assume their short-range values for all d, if $\sigma_{int}>2$. These phenomena assert that the magnetic moments in the present system interact with one another through long-range interactions, which decay faster than $1/a^5$. This assumption together with the Rhodes-Wohlfarth criterion suggest that the present series of amorphous alloys are *weak itinerant* ferromagnet. The critical exponents obtained from the magnetoresistivity data[19] analysis near the critical region also support the present results. The result of the present analysis clearly distinguishes between the effective and asymptotic critical exponents [Fig. 3(b)] for the present samples and also for a few published data. An extension of this work to various published data[5] on different samples can help further in identifying the main source of the spread in the reported exponent values.

In summary, a systematic and detailed investigation of the critical behavior of *weak itinerant* ferromagnet $Fe_{90-x}Mn_xZr_{10}$ alloys by various methods is presented. The detailed analysis results in the nonanalytic correction terms arising from nonlinear irrelevant scaling fields dominating over the analytic ones in the asymptotic critical region but the reverse is true for temperatures outside the ACR. Based on our observations, we conclude that the T_c remarks the temperature at which the transition from the paramagnetic state to a state with long-range ferromagnetic order takes place. The obtained results provide strong experimental evidence of *weak itinerant* ferromagnetism in the glassy alloys in question.

We thank Professor R. A. Dunlap and Professor V. V. Rao for valuable discussions. One of the authors (A.P.) would like to thank the Council of Scientific and Industrial Research (CSIR), New Delhi, India, for providing financial support for this work.

*Present address: Department of Physics and Center for Nanospinics of Spintronic Materials, Korea Advanced Institute of Science and Technology (KAIST), Taejeon, Korea.

†Electronic address: veeturi@phy.iitkgp.ernet.in

[1] L. J. de Jongh, in *Magnetic Phase Transitions*, edited by M. Ausloos and R. J. Elliott (Springer-Verlag, Berlin, 1983), p. 172; A. Coniglio, *ibid*., p. 195; Phys. Rev. Lett. **46**, 250 (1981); Anita G. Bernat, X. Chen, H. P. Kunkel, and Gwyn Williams, Phys. Rev. B **52**, 10 160 (1995).

[2] T. C. Lubensky, Phys. Rev. B **11**, 3573 (1975); A. Weinrib and B. I. Halprin, Phys. Rev. B **27**, 413 (1983); G. Jug, *ibid.* **27**, 609 (1983); H. O. Heuer and D. Wagner, *ibid.* **40**, 2502 (1989).

[3] A. B. Harris, J. Phys. C **7**, 1671 (1974).

[4] P. D. Babu and S. N. Kaul, J. Phys.: Condens. Matter **9**, 7189 (1997); M. Charalambous, O. Riou, P. Gandit, B. Billon, P. Lejay, J. Chaussy, W. N. Hardy, D. A. Bonn, and Ruixing Liang, Phys. Rev. Lett. **83**, 2042 (1999); T. Kise, T. Ogasawara, M. Ashida, Y. Tomioka, Y. Tokura,and M. Kuwata-Gonokami, *ibid.* **85**, 1986 (2000); F. Y. Yang, C. L. Chien, X. W. Li, Gang Xiao, and A. Gupta, Phys. Rev. B **63**, 092403 (2001); K. Balakrishnan and S. N. Kaul, *ibid.* **65**, 134412 (2002).

[5] H. Yamamoto, H. Onodora, K. Hosoyama, T. Masumoto, and H. Yamauchi, J. Magn. Magn. Mater. **31-34**, 1579 (1983); H. Yamauchi, H. Onodora, and H. Yamamoto, J. Phys. Soc. Jpn. **53**, 747 (1984); K. Winschuh and M. Rosenberg, J. Appl. Phys. **61**, 4401 (1987); G. K. Nicolaides, G. C. Hadjipanayis, and K. V. Rao, Phys. Rev. B **48**, 12 759 (1993); I. Abu-Aliarayesh and M. R. Said, J. Magn. Magn. Mater. **210**, 73 (2000); G. D. Mukherjee, S. Chakraborty, D. D. Rathnayaka, D. G. Naugle, and A. K. Majumdar, *ibid.* **214**, 185 (2000).

[6] A. Aharony and M. E. Fisher, Phys. Rev. B **8**, 3323 (1973); E. Frey and F. Schwabl, Phys. Rev. B **43**, 833 (1991).

[7] M. E. Fisher, S. K. Ma, and B. G. Nickel, Phys. Rev. Lett. **29**, 917 (1972); J. Sak, Phys. Rev. B **8**, 281 (1973).

[8] G. S. Joyce, Phys. Rev. **146**, 349 (1966).

[9] J. S. Kouvel and J. B. Cowly, in *Critical Phenomena in Alloys*,

Magnets and Superconductors, edited by R. E. Mills, E. Ascher, and R. I. Jaffee (McGraw-Hill, New York, 1971), p. 437; R. Jesser, A. Bieber, and R. Kuentzler, J. Phys. (Paris) **44**, 631 (1983); M. Seeger, H. Kronmuller, and H. J. Blythe, J. Magn. Magn. Mater. **139**, 312 (1995).

[10] A. Perumal, V. Srinivas, A. Dhar, V. V. Rao, and R. A. Dunlap, Phys. Status Solidi A **178**, 783 (2000); A. Perumal, V. Srinivas, V. V. Rao, and R. A. Dunlap (unpublished).

[11] A. Perumal, Ph.D thesis, Indian Institute of Technology, Kharagpur, India, 2002.

[12] J. S. Kouvel and M. E. Fisher, Phys. Rev. **136**, B1626 (1964).

[13] η_{cross} denotes the crossover reduced temperature at which the critical exponent values are observed to vary significantly; see A. Perumal, V. Srinivas, V. V. Rao, and R. A. Dunlap, Physica B **292**, 164 (2000).

[14] A. Perumal, V. Srinivas, K. S. Kim, S. C. Yu, V. V. Rao, and R. A. Dunlap, Phys. Rev. B **65**, 064428 (2002).

[15] G. S. Cargill III, in *Solid State Physics*, edited by H. Ehrenrich, F. Seitz, and D. Turnbill (Academic, New York, 1975), Vol. 30, p. 227.

[16] The high-field region of the low-temperature σ-H curve is analyzed with an analytical expression $\sigma(H)=\chi_{hf}H+\sigma_0(1-\epsilon H^{-\phi})$, where χ_{hf} is the high-field susceptibility and ϵ is the local magnetic anisotropy. More details are given in Ref. 14. χ_{dc}^{-1} is the inverse susceptibility data, computed from the intercept values at different temperatures on the abscissa ($T \geqslant T_c$), when the linear high-field portion of the MAP plot is extrapolated to $(H/\sigma)^{1/\gamma}=0$. χ_{ac}^{-1} is the inverse susceptibility data obtained from low-field ac susceptibility measurements. h_0 and m_0 are asymptotic critical amplitudes.

[17] S. N. Kaul, V. Siruguri, and G. Chandra, Phys. Rev. B **45**, 12 343 (1992).

[18] E. P. Wohlfarth, J. Magn. Magn. Mater. **7**, 113 (1978); T. Moriya, *ibid.* **31-34**, 10 (1983).

[19] A. Perumal, V. Srinivas, A. K. Nigam, G. Chandra, and R. A. Dunlap (unpublished).